Asymptotic Behavior of Cold Superdense Stars

B. KENT HARRISON*
Los Alamos Scientific Laboratory, Los Alamos, New Mexico
(Received 13 July 1964; revised manuscript received 30 November 1964)

The behavior of superdense ("neutron") stars at absolute zero has been studied. It is shown that, with certain assumptions about the equation of state, the mass and radius of such a star approach constants in an oscillatory fashion as the star's central density increases. The assumptions about the equation of state are: $dP/d\rho>0$ everywhere, and for sufficiently high-density ρ, the pressure divided by the density P/ρ approaches a constant. These assumptions are physically reasonable, especially if one assumes a real speed of sound which is finite, but always less than the speed of light. The results of the paper show that there exists for such stars an infinite series of ranges of the central density, in which ranges $dM/d\rho_0$ alternates in sign, where M is the total star mass and ρ_0 is the central density. This indicates alternate local stability and instability; however, the total binding energy is positive for ρ_0 greater than $\sim 10^{16}$ g/cm^3, so that instability against large-scale deformation exists. A striking feature of the results of this paper is that their qualitative nature does not depend on whether or not the general relativistic form of the equations is used. The exact quantitative results do, of course, depend on the form of the equations, as well as on the exact equation of state used.

1. INTRODUCTION

THE properties of stars of extremely high density (on the order of nuclear mass densities or higher) were first investigated by Landau[1] and by Oppenheimer, Serber, and Volkoff.[2,3] There has recently been renewed interest in such superdense stars, partly as a matter of principle[4,5] and partly because of astronomical observations indicating possible existence of such objects.[6,7] To investigate such stars, one needs an equation of state. Various equations of state have been proposed for such high densities,[4,8,9] and calculations using these equations of state have been performed,[4] but there is no agreement as to which equation is most appropriate. It therefore behooves us to investigate such properties of superdense stars which are relatively insensitive to the choice of equation of state. An initial investigation into such properties has been conducted by Misner and Zapolsky,[10] who show that, if a polytropic equation of state is assumed for high densities, there is a maximum mass which can exist for cold static equilibrium, and that dynamically stable stars can exist with masses below this maximum. The present paper extends this result and shows that, under certain simple assumptions concerning the equation of state, the mass and radius of a superdense star approach constant values in an oscillatory fashion as the central density is increased. This shows that there exists an infinite series of ranges of the central density in which ranges $dM/d\rho_0$ alternates in sign, where M is the total star mass and ρ_0 is its central density. Thus, there is alternate local stability and instability of the star; however, the total binding energy becomes positive at $\rho_0\sim 10^{16}$ g/cm^3 and remains so for larger ρ_0 so that the star is unstable against large-scale deformation above this point.

Many of the results of this paper have been derived by Wheeler by alternate methods.[11] Also given in this reference[11] is a detailed analysis of the problems of stability for superdense stars and of baryon conservation, which are beyond the scope of the present paper.

2. HYDROSTATIC EQUATIONS FOR THE COLD STAR IN EQUILIBRIUM

We consider first the equations derived from general relativity. If we use a metric in the Schwarzschild form,

$$ds^2=e^{\nu}c^2dt^2-e^{\lambda}dr^2-r^2(d\theta^2+\sin^2\theta d\phi^2)\,, \qquad (2.1)$$

we get the hydrostatic equations[3]

$$\frac{dP}{dr}=-\frac{G(Pc^{-2}+\rho)(M+4\pi r^3Pc^{-2})}{r(r-2GMc^{-2})}\,, \qquad (2.2)$$

$$dM/dr=4\pi r^2\rho\,, \qquad (2.3)$$

where P is the pressure, ρ is the density, r is the radius, M is the mass inside the radius r, and G is the gravitational constant. The equation of state is

$$P=P(\rho)\,. \qquad (2.4)$$

We take the temperature to be at absolute zero, as

---

* Present address: Physics Department, Brigham Young University, Provo, Utah.

1 L. Landau, Phys. Z. Sowjetunion **1**, 285 (1932).

2 J. R. Oppenheimer and R. Serber, Phys. Rev. **54**, 540 (1938).

3 J. R. Oppenheimer and G. Volkoff, Phys. Rev. **55**, 374 (1939).

4 B. K. Harrison, M. Wakano, and J. A. Wheeler, in Onzieme Conseil de l'Institut International de Physique Solvay, *La Structure et l'Evolution de l'Universe* (Editions Stoops, Brussels, 1958); see also J. A. Wheeler in *Gravitation and Relativity*, edited by H.-Y. Chiu and W. F. Hoffman (W. A. Benjamin Inc., New York, 1964), Chap. 10.

5 H.-Y. Chiu and E. E. Salpeter, Phys. Rev. Letters **12**, 413 (1964).

6 D. C. Morton, Nature **201**, 1308 (1964).

7 H.-Y. Chiu, Ann. Phys. (N. Y.) **26**, 364 (1964).

8 T. H. R. Skyrme, Nucl. Phys. **9**, 615 (1959); A. G. W. Cameron, Astrophys. J. **130**, 884 (1959).

9 Ya. B. Zel'dovich, Zh. Eksperim. i Teor. Fiz. **41**, 1609 (1961) [English transl.: Soviet Phys.—JETP **14**, 1143 (1962)].

10 C. W. Misner and H. S. Zapolsky, Phys. Rev. Letters **12**, 635 (1964).

11 B. K. Harrison, K. S. Thorne, M. Wakano, and J. A. Wheeler, *Gravitational Collapse and Baryon Conservation* (University of Chicago Press, Chicago, Illinois, to be published).

noted before. We define new variables as

$$m=c^{-2}GM\,, \tag{2.5a}$$

$$S=c^{-4}GP\,, \tag{2.5b}$$

$$D=c^{-2}G\rho\,; \tag{2.5c}$$

then Eqs. (2.2)–(2.4) become

$$\frac{dS}{dr}=-\frac{(D+S)(m+4\pi r^3S)}{r(r-2m)}\,, \tag{2.6}$$

$$dm/dr=4\pi Dr^2\,, \tag{2.7}$$

$$S=S(D)\,. \tag{2.8}$$

The boundary conditions are

$$r=0:\quad m=0,\quad D=D_0\,, \tag{2.9}$$

$$r=R:\quad D=\bar{D}(=G\bar{\rho}c^{-2})\,. \tag{2.10}$$

R is the radius of the star; the outer edge of the star may be assumed to have density $\bar{\rho}$ (the density of iron, say). $\bar{D}$ is very small.

We assume the following facts about the equation of state:

$$dS/dD>0\,, \tag{2.11}$$

$$\lim_{D\to\infty} S/D=k,\quad 0<k\leq 1\,. \tag{2.12}$$

Here k is a constant, necessarily positive; it must also be at most unity, since the speed of sound cannot exceed the speed of light. If we have $P\sim n^\gamma$ (n=baryon number density), then $k=\gamma-1$. A further assumption is given at the end of Sec. 3.

Equations (2.11) and (2.12) are very plausible physically. If $dS/dD<0$ anywhere, we have an imaginary speed of sound, so that sound waves are not propagated at all. If $S\to\alpha D^\beta$, $\beta\neq 1$, as $D\to\infty$, the speed of sound will be proportional to $D^{(\beta-1)/2}$. If $\beta>1$, the speed of sound becomes infinite as $D\to\infty$, which contradicts relativity; and if $\beta<1$, the speed of sound goes to zero as $D\to\infty$. This seems very unlikely, although conceivably it could happen.

If we neglect S compared to D, $4\pi r^3S$ compared to m, and $2m$ compared to r in the right-hand side of Eq. (2.6), we obtain the nonrelativistic equation of hydrostatic pressure balance:

$$dS/dr=-Dm/r^2\,. \tag{2.13}$$

We can also use an equation intermediate between Eqs. (2.6) and (2.13):

$$dS/dr=-(D+S)m/r^2\,. \tag{2.14}$$

The results we obtain will actually be independent of which form is used; we will work with Eq. (2.14) [or (2.13)] and will then extend the results to Eq. (2.6).

We shall need some of the terms in the expansions of m, D, and S for small r. From Eqs. (2.6)–(2.9), we get

$$m=\frac{4\pi D_0}{3}r^3-\frac{8\pi^2}{5S'(D_0)}[D_0+S(D_0)]\times[\tfrac{1}{3}D_0+S(D_0)]r^5+O(r^7)\,, \tag{2.15}$$

$$D=D_0-(2\pi/S'(D_0))[D_0+S(D_0)]\times[\tfrac{1}{3}D_0+S(D_0)]r^2+O(r^4)\,, \tag{2.16}$$

$$S=S(D_0)-2\pi[D_0+S(D_0)]\times[\tfrac{1}{3}D_0+S(D_0)]r^2+O(r^4)\,, \tag{2.17}$$

where $S'(D)\equiv dS/dD$. If Eq. (2.13) is used instead of Eq. (2.6), we must neglect $S(D_0)$ compared with D_0.

3. TRANSFORMATIONS OF THE EQUATIONS; IDEAL CASE

If we combine Eqs. (2.6) and (2.8) we get

$$\frac{dD}{dr}\frac{dS}{dD}=-\frac{(D+S)(m+4\pi r^3S)}{r(r-2m)}\,. \tag{3.1}$$

We define

$$g(D)=\frac{k}{1+k}\left(\frac{D+S}{DS'}\right), \tag{3.2}$$

$$h(D)=S(D)/D\,. \tag{3.3}$$

Then Eq. (3.1) becomes

$$\frac{dD}{dr}=-\left(\frac{1+k}{k}\right)\frac{Dg(D)[m+4\pi r^3Dh(D)]}{r(r-2m)}\,. \tag{3.4}$$

$g(D)$ has been chosen so that

$$\lim_{D\to\infty} g(D)=1\,. \tag{3.5}$$

Equation (2.14) now becomes

$$\frac{dD}{dr}=-\left(\frac{1+k}{k}\right)\frac{Dg(D)m}{r^2}\,. \tag{3.6}$$

We define

$$f(D)\equiv k/S'\,; \tag{3.7}$$

then

$$\lim_{D\to\infty} f(D)=1 \tag{3.8}$$

and Eq. (2.13) becomes

$$\frac{dD}{dr}=-\frac{1}{k}\frac{Df(D)m}{r^2}\,. \tag{3.9}$$

We now temporarily introduce a very special case, here called the "ideal" case. In this case we assume an "ideal" equation of state

$$S=kD \tag{3.10}$$

everywhere. This yields $f=1$, $g=1$, $h=k$. It now becomes apparent that we can transform the equations so as to remove the explicit r dependence. The most convenient way to do this is to introduce the variables

$$\nu=m/r, \tag{3.11}$$

$$\sigma=4\pi r^3D/3m. \tag{3.12}$$

Then Eq. (2.7) becomes

$$(r/3)(d\nu/dr)=\nu(\sigma-\tfrac{1}{3}), \tag{3.13}$$

and the alternate forms of the pressure equations, Eqs. (3.4), (3.6), and (3.9), become, respectively,

$$\frac{r}{3}\frac{d\sigma}{dr}=\sigma\left[1-\sigma-\frac{(1+k)\nu(1+3k\sigma)}{3k(1-2\nu)}\right], \tag{3.14}$$

$$\frac{r}{3}\frac{d\sigma}{dr}=\sigma\left[1-\sigma-\left(\frac{1+k}{3k}\right)\nu\right], \tag{3.15}$$

$$\frac{r}{3}\frac{d\sigma}{dr}=\sigma\left[1-\sigma-\left(\frac{1}{3k}\right)\nu\right]. \tag{3.16}$$

If now

$$r=ae^{x/3}, \tag{3.17}$$

where a is a suitably chosen standard length, the operator $\frac{1}{3}rd/dr$ becomes simply d/dx.

We now see that the transformations (3.11), (3.12), and (3.17) aid in simplifying the equations. Let us apply them to the exact equations, Eqs. (2.7) and (3.4), (3.6), or (3.9). We get, respectively,

$$d\nu/dx=\nu(\sigma-\tfrac{1}{3}), \tag{3.18}$$

$$\frac{d\sigma}{dx}=\sigma\left[1-\sigma-\left(\frac{1+k}{3k}\right)\nu g(D)\left(\frac{1+3\sigma h(D)}{1-2\nu}\right)\right], \tag{3.19}$$

$$\frac{d\sigma}{dx}=\sigma\left[1-\sigma-\left(\frac{1+k}{3k}\right)\nu g(D)\right], \tag{3.20}$$

$$\frac{d\sigma}{dx}=\sigma\left[1-\sigma-\frac{1}{3k}\nu f(D)\right], \tag{3.21}$$

with

$$D=3\nu\sigma(4\pi a^2)^{-1}e^{-2x/3}. \tag{3.22}$$

For the ideal case, these equations reduce to Eqs. (3.13)–(3.16).

Near $r=0$ ($x=-\infty$) we have for the exact case

$$\nu=\tfrac{4}{3}\pi D_0a^2e^{2x/3}+\cdots, \tag{3.23}$$

$$\sigma=1-4\pi a^2(1+k)(15k)^{-1}D_0g(D_0)\times[1+3h(D_0)]e^{2x/3}+\cdots. \tag{3.24}$$

We drop the $3h(D_0)$ if we use the intermediate equation, and further replace $1+k$ by 1 if we use the usual hydrostatic equation.

We need some information about the nature of f, g, and h as functions of D. A possible $h(D)$ is given in Ref. 4 and is monotonic except for a small region near $\rho=10^{12}$ g/cm^3 ($D\simeq7\times10^{-17}$ cm^{-2}). Inspection of this equation indicates that both f and g are very large for small D and decrease monotonically except for a small region near $D=7\times10^{-17}$ cm^{-2} (see above), approaching unity from the upward side for large D. We assume this qualitative behavior for f and g (descent to unity, monotonic for large enough D) to hold for all possible equations of state.

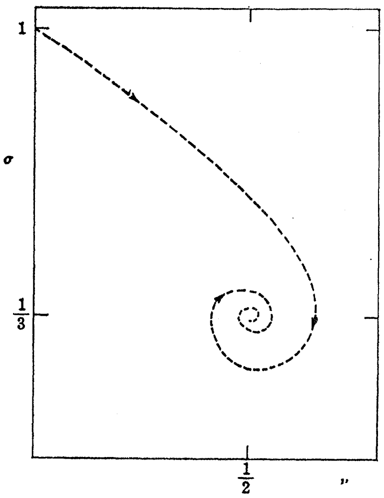

FIG. 1. Qualitative sketch of phase plane trajectory for ideal equation of state. Convergent focal behavior is apparent. The focus has been fixed at $\sigma=\frac{1}{3}$, $\nu=\frac{1}{2}$.

4. PHASE PLANE ANALYSIS; APPROXIMATE EQUATIONS

We now work with Eqs. (3.18) and (3.20). Consider first the ideal case, with $f=g=1$. Then Eq. (3.20) or (3.21) may be written

$$d\sigma/dx=\sigma(1-\sigma-\lambda\nu), \tag{4.1}$$

where $\lambda=(1+k)(3k)^{-1}$ or $(3k)^{-1}$, respectively. Combination of Eqs. (3.18) and (4.1) yields

$$\frac{d\sigma}{d\nu}=\frac{\sigma(1-\sigma-\lambda\nu)}{\nu(\sigma-\frac{1}{3})}. \tag{4.2}$$

Equations (3.23) and (3.24) can be used to obtain boundary conditions:

$$x=-\infty:\quad \nu=0,\quad \sigma=1,\quad d\sigma/d\nu=-\tfrac{3}{5}\lambda. \tag{4.3}$$

We may now use the phase plane analysis of nonlinear mechanics.[12] We take the $\nu-\sigma$ plane to be our phase plane. We find the critical points—points at which $d\sigma/d\nu$ is indeterminate—and determine their nature. There are three critical points: $\sigma=0$, $\nu=0$ is a saddle point; $\sigma=1$, $\nu=0$ is a saddle point; $\sigma=\frac{1}{3}$, $\nu=\frac{2}{3}\lambda^{-1}$ is a stable focus. The trajectory of interest begins at the

[12] For example, see S. Lefschetz, *Differential Equations: Geometric Theory* (Interscience Publishers, Inc., New York, 1957), Chap. IX; N. Minorsky, *Nonlinear Oscillations* (D. Van Nostrand & Company, Princeton, New Jersey, 1962), Chap. 1.

critical point $\sigma=1$, $\nu=0$ with negative slope and moves toward the focus at $\sigma=\frac{1}{3}$, $\nu=\frac{2}{3}\lambda^{-1}$, eventually spiralling towards the focus. The phase plane plot of this trajectory is shown in Fig. 1. The arrows point in the direction of increasing x. At the point $\sigma=1$, $\nu=0$, $x=-\infty$; x increases from this value, at a rate determined by D_0, and would reach $+\infty$ at $\sigma=\frac{1}{3}$, $\nu=\frac{2}{3}\lambda^{-1}$ except for the fact that the trajectory stops when $D=\bar{D}$. The x value when this happens is related to the final radius R. We might expect the stopping point to be very close to the focus, so the rough final values are

$$\sigma=\tfrac{1}{3}, \quad \nu=\tfrac{2}{3}\lambda^{-1}. \tag{4.4}$$

From Eqs. (3.11) and (3.12), with $r=R$ and $D=\bar{D}$, we get

$$m(R)=2R/3\lambda, \tag{4.5a}$$

$$4\pi R^2\bar{D}=2/3\lambda. \tag{4.5b}$$

Thus, the star's radius is given asymptotically by

$$R=(6\pi\lambda\bar{D})^{-1/2} \tag{4.6}$$

and the star's asymptotic mass is

$$m(R)=2(3\lambda)^{-1}(6\pi\lambda\bar{D})^{-1/2}. \tag{4.7}$$

These values are approximate and hold only for the ideal case, so they will deviate considerably from values calculated with exact equations of state.

We can obtain the behavior of σ and ν near the focus by writing

$$\bar{\sigma}=\sigma-\tfrac{1}{3}, \tag{4.8}$$

$$\bar{\nu}=\nu-\tfrac{2}{3}\lambda^{-1}, \tag{4.9}$$

and assuming $\bar{\sigma}$ and $\bar{\nu}$ small. We find

$$\bar{\nu}=Ae^{-x/6}\sin[\tfrac{1}{6}(\sqrt{7})x+\epsilon] \tag{4.10}$$

and

$$\bar{\sigma}=\tfrac{1}{4}\lambda Ae^{-x/6}\{-\sin[\tfrac{1}{6}(\sqrt{7})x+\epsilon] +(\sqrt{7})\cos[\tfrac{1}{6}(\sqrt{7})x+\epsilon]\}, \tag{4.11}$$

where A and ϵ are determined by the previous trajectory and are functions of D_0. For large x, $\bar{\sigma}$, and $\bar{\nu}$ are small. If we return to the original variables and put $r=R$, $D=\bar{D}$, we have

$$\frac{m(R)}{R}=\frac{2}{3\lambda}+A\left(\frac{a}{R}\right)^{1/2}\sin\left(\frac{(\sqrt{7})}{2}\ln\frac{R}{a}+\epsilon\right), \tag{4.12}$$

$$\frac{4\pi R^3\bar{D}}{3m(R)}=\tfrac{1}{3}+\frac{\lambda A}{4}\left(\frac{a}{R}\right)^{1/2}\left[-\sin\left(\frac{(\sqrt{7})}{2}\ln\frac{R}{a}+\epsilon\right) +(\sqrt{7})\cos\left(\frac{(\sqrt{7})}{2}\ln\frac{R}{a}+\epsilon\right)\right]. \tag{4.13}$$

The oscillatory terms are small and so we can solve these equations for R and $m(R)$ by successive approximation. If we take Eq. (4.6) for R and substitute it into the oscillatory terms, we get corrected values for R and $m(R)$. We now note an important feature: as D_0 changes, ϵ changes, and the correction terms oscillate. It becomes apparent, then, that R and $m(R)$ oscillate as D_0 changes. For this behavior to be apparent, D_0 must be high enough that when the edge of the star is reached, the trajectory has begun to spiral around the focus.

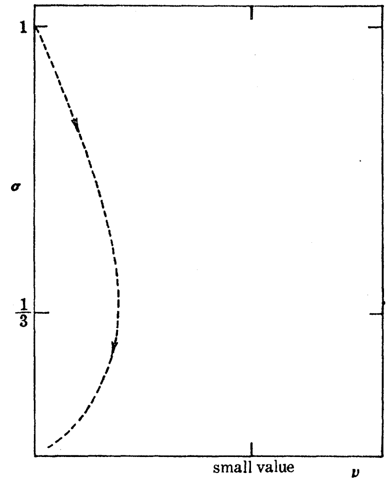

FIG. 2. Qualitative sketch of phase-plane trajectory for actual equation of state for low-central density. Trajectory converges rapidly to neighborhood of origin.

We may get some idea of the behavior of A and ϵ with D_0 by putting $\sigma=\frac{1}{3}$, $\nu=\frac{2}{3}\lambda^{-1}$ in Eq. (3.22). This gives

$$D=(6\pi\lambda a^2)^{-1}e^{-2x/3}, \tag{4.14}$$

so that

$$x=-\tfrac{3}{2}\ln D+\text{const}. \tag{4.15}$$

We now treat the whole trajectory as a spiral, so that we can use Eqs. (4.10) and (4.11) everywhere, and can take $\sigma=1$, $\nu=0$ at $D=D_0$. This yields, after some computation

$$(\tfrac{1}{6}\sqrt{7})x+\epsilon=(\tfrac{1}{4}\sqrt{7})\ln(D_0/D)-\sin^{-1}(\tfrac{1}{4}\sqrt{7}). \tag{4.16a}$$

It is now clear that the oscillation in R and $m(R)$ with D_0 has a constant period $T=8\pi/\sqrt{7}$ if $\ln D_0$ is taken to be the variable. This behavior actually is not precisely met because Eqs. (4.10) and (4.11) do not hold for the entire trajectory.

We also find for this simplified model that

$$A=8[(3\sqrt{7})\lambda]^{-1}D_0^{-1/4}. \tag{4.16b}$$

Our argument is incomplete, because we have not shown that the trajectory with the actual equation of state—instead of the ideal one given by Eq. (3.10)—behaves as we have shown. When we investigate the case using the exact equation of state, we find important differences; however, we still obtain the oscillatory dependence of R and $m(R)$ on D_0.

We first note that, at $x=-\infty$ $(r=0)$, Eqs. (3.23) and (3.24) yield $\nu=0$, $\sigma=1$, and $d\sigma/d\nu=-\frac{3}{5}\lambda g(D_0)$, where $\lambda=(1+k)(3k)^{-1}$. Thus, the trajectory in the ν-σ phase plane begins much the same as before. However, since $g>1$, we note that the new slope is less (i.e., more

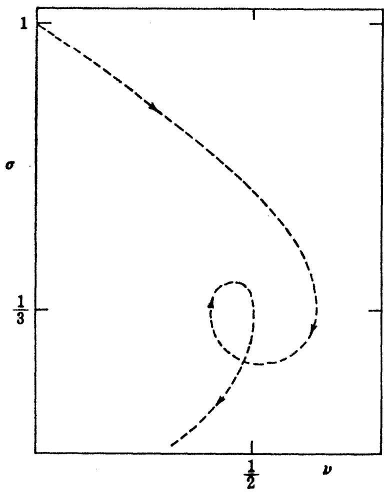

FIG. 3. Qualitative sketch of phase-plane trajectory for actual equation of state for high-central density. Trajectory spirals, as in ideal case, and then develops a "tail."

negative) than the slope in the ideal case. Thus, the new curve plunges more steeply from $\nu=0$, $\sigma=1$ than before.

In particular, for small and intermediate D, $g(D)$ is very large. The last term in Eq. (3.20) will completely dominate, so that this equation becomes

$$d\sigma/dx=-\lambda\sigma\nu g(D). \qquad (4.17)$$

Thus, σ decreases at a very rapid rate. From Eq. (3.18), we see that ν increases until $\sigma=\frac{1}{3}$ and then decreases. The final values of σ and ν (determined by $D=\bar{D}$) will be very close to zero. The trajectory will have the appearance of Fig. 2.

As we increase D_0, g approaches unity, and the initial slope of the trajectory approaches that of the ideal case more closely. For large D_0, g will remain close to 1 for a considerable distance along the trajectory, which will approximate the ideal case for some distance and will perform one or more loops. The critical "point" now occurs at $\nu=2/[3\lambda g(D)]$; this gradually moves to the left as D decreases and g moves away from 1, so that the spirals as a whole move gradually to the left.

Eventually, however, D becomes small and g becomes large. The term involving g begins to dominate, and Eq. (4.14) applies again. σ can no longer increase, and the trajectory crosses the spirals and again moves toward the origin. However, ν has reached an appreciable value (of the order of unity) in the first part of the trajectory, so that its final value will be larger than the final value for small initial D. The trajectory may appear as in Fig. 3, although for higher D_0 there will be more spirals.

We must now ask about the behavior of the final values of σ and ν. It is apparent that, as D_0 increases, the total length of the trajectory will increase and that the place where the trajectory begins its last downward plunge will vary in position around the spiral. We may call the last part of the trajectory the "tail." The increased length of the trajectory will primarily be taken up in the spiral and will cause differences in position of the tail.

To fix ideas, suppose that at the last horizontal tangent in Fig. 3, the value of D is D_1. Roughly at this point $g(D)$ becomes large enough to begin domination of the $d\sigma/dx$ equation. If we now increase D_0 slightly, the point at which $D=D_1$ will move a slight distance clockwise around the spiral. This will cause the entire tail of the trajectory to shift slightly downwards and to the right. As D_0 increases, the point $D=D_1$ will continue to move clockwise along the spiral. The trajectory will gain added length, most of which will go to forming more spiral. As D_0 increases, the point $D=D_1$ will pass a horizontal tangent below the line $\sigma=\frac{1}{3}$, as shown in Fig. 4. Further increase in D_0 will produce a second loop in the spiral, as in Fig. 5.

We can now see that, as D_0 increases, the point $D=D_1$ will travel around the spiral, converging toward the center. The final point on the trajectory will map out a spiral as $D=D_1$ does.

The following is now apparent. We may select a value of D_0, called a "threshold" value, such that for all D_0 above this value, a spiral is formed in the trajectory. (There is thus considerable arbitrariness in definition of this threshold.) For any D_0 above this threshold, the first part of the trajectory forms a spiral, the second part a tail which begins in the central region of the spiral and ends near the ν axis. One essential feature of the tail is that it begins in a small, bounded region of the ν-σ plane, which is roughly a neighborhood of the quasicritical point $\sigma=\frac{1}{3}$, $\nu=\frac{2}{3}\lambda^{-1}$. (This neighborhood has moved slightly to the left because of the gradual increase in g.) Another essential feature is the fact that the tail always begins roughly at the same value of $D(\simeq D_1)$, nearly irrespective of D_0. The value of D_0, if above threshold, primarily determines the number of circuits in the spiral and performs the important function of determining the "phase" where the tail begins.

We now note from these facts and Eq. (3.22) that the value of x where the tail begins is also roughly independent of D_0. The tail thus begins at approximately the same values of σ, ν, and x for every D_0 above

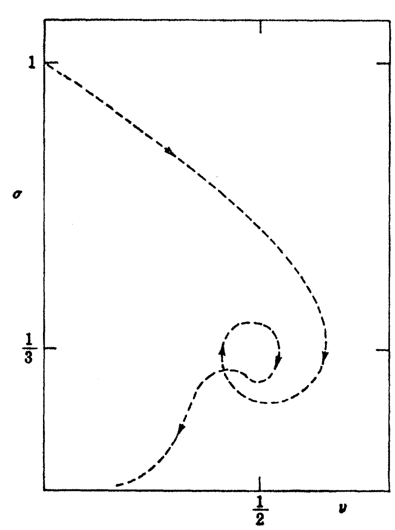

FIG. 4. Effect of increasing central density from value used in Fig. 3. Trajectory develops two additional horizontal tangents; final point moves to the left.

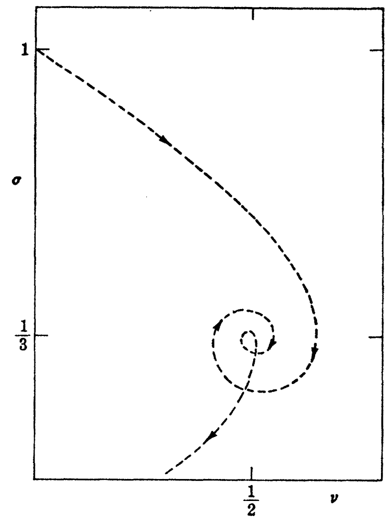

FIG. 5. Effect of increasing central density from value used in Fig. 4. Trajectory develops additional loop in spiral; final point moves back to the right.

threshold. The major variations of the tail's initial point are found in the small oscillations of σ and ν at $D=D_1$ for varying D_0. These are transmitted to the final point of the tail.

We can add some rigor to the above qualitative argument by the following treatment. Let us consider the tail, which begins from the point at which $D=D_1$ (now called the "initial" point) and continues until $D=\bar{D}$. We write $\sigma=\sigma_1$ and $\nu=\nu_1$ at this point. The "initial" x at this point can now be determined from Eq. (3.22). Let us write the functions $\sigma(x)$ and $\nu(x)$ on this special trajectory as $\sigma^*(x)$ and $\nu^*(x)$, so that

$$d\nu^*/dx=\nu^*(\sigma^*-\tfrac{1}{3}) \tag{4.18}$$

and

$$d\sigma^*/dx=\sigma^*[1-\sigma^*-\lambda\nu^*g(D^*)], \tag{4.19}$$

with

$$D^*=3\nu^*\sigma^*(4\pi a^2)^{-1}e^{-2x/3}. \tag{4.20}$$

Now consider a trajectory corresponding to a slightly different value of D_0, and use the usual variables ν and σ to describe it. We define

$$\Delta\sigma(x)=\sigma(x)-\sigma^*(x), \tag{4.21}$$

$$\Delta\nu(x)=\nu(x)-\nu^*(x). \tag{4.22}$$

Now, our equations and their derivatives are all continuous in the region of the tail, so the new trajectory will be close to the old one. In fact, for large enough D_0, the spiral will be tight enough, and the two trajectories so close, that we can neglect squares of $\Delta\sigma$ and $\Delta\nu$ along the trajectory. We may now compute the derivatives of $\Delta\sigma$ and $\Delta\nu$, neglecting terms of order higher than the first:

$$d(\Delta\nu)/dx=(\Delta\nu)(\sigma^*-\tfrac{1}{3})+(\Delta\sigma)\nu^*, \tag{4.23}$$

$$d(\Delta\sigma)/dx=(\Delta\nu)\lambda\sigma^*(g^*+D^*g^{*\prime}) + (\Delta\sigma)[1-2\sigma^*+\lambda\nu^*(g^*+D^*g^{*\prime})], \tag{4.24}$$

where $g^*=g(D^*)$. We now have two coupled linear equations for $\Delta\nu$ and $\Delta\sigma$, with coefficients as given functions of x (ν^* and σ^* are fixed once and for all). The coefficients are also independent of the position of the tail's initial point in the spiral and of the initial value of x, to lowest order; as pointed out earlier, these quantities are approximately constant at the beginning of the tail. Equations (4.23) and (4.24) may be called "variation" equations.

We may now use the variation equations to calculate $\Delta\sigma$ and $\Delta\nu$ from $D=D_1$ to $D=\bar{D}$. Because the variation equations are linear, $\Delta\sigma$ and $\Delta\nu$ (final) will be linear combinations of $\Delta\sigma$ and $\Delta\nu$ (initial). In other words, the variation equations provide a linear mapping of possible initial points into final points.

The positions of the "initial" points may be given approximately by Eqs. (4.10) and (4.11), in which x is roughly constant and A and ϵ vary with D_0. (This variation is given explicitly earlier in this section.) The locus of these initial points is a spiral, qualitatively the same as the earlier spiral, although the variable is now actually D_0 instead of x. The linear mapping maps this spiral into another spiral, the locus of the final points. (This can be seen qualitatively by considering the initial spiral as a set of nested ellipses; the mapping converts this set into another set of nested ellipses.) Thus we see that the final point moves in a convergent spiral as D_0 increases. We see also that the period of oscillation with $\ln D_0$ as variable remains the same as before, as does the amplitude. The essential feature in all these conclusions is the fact that the initial σ, ν, and x are roughly the same for each "tail."

The above discussion shows what was to be proved: that R and $m(R)$ vary in an oscillatory fashion with D_0 for large enough D_0. A graph of R *versus* $m(R)$, with D_0 varying along the curve, will show a spiral-like behavior. [It may be argued that a spiral will not occur if R and $m(R)$ are exactly in phase; however, in that case, $\nu=m/r$ would not oscillate, and it does.]

The behavior will be the same if we use Eq. (3.21) instead of (3.20), since $f(D)$ is similar to $g(D)$ in all important features.

5. GENERAL RELATIVISTIC CASE

We use the exact Eqs. (3.18) and (3.19). If we consider first the ideal case, we find critical points in the ν-σ plane as follows: saddle points at $\sigma=0$, $\nu=0$; $\sigma=1$, $\nu=0$; and $\sigma=0$, $\nu=\frac{1}{2}$; node at $\sigma=-(3k)^{-1}$, $\nu=\frac{1}{2}$; stable focus at $\sigma=\frac{1}{3}$, $\nu=2k(k^2+6k+1)^{-1}$. A phase-plane plot shows that the trajectory appears much as before (Fig. 1), with one qualification: the trajectory can never move as far right as the line $\nu=\frac{1}{2}$. This means that $1-2\nu>0$ always, and shows that the Schwarzschild radius for every mass $m(r)$ lies inside the mass.

We now investigate the case with the exact equation of state. We first note that the above conclusion concerning the Schwarzschild radius still holds for $g>0$, i.e., for $dS/dD>0$. Suppose ν begins to approach $\frac{1}{2}$. Then Eq. (3.19) yields a large negative $d\sigma/dx$, σ decreases rapidly, and $d\nu/dx$ goes negative so that ν begins to

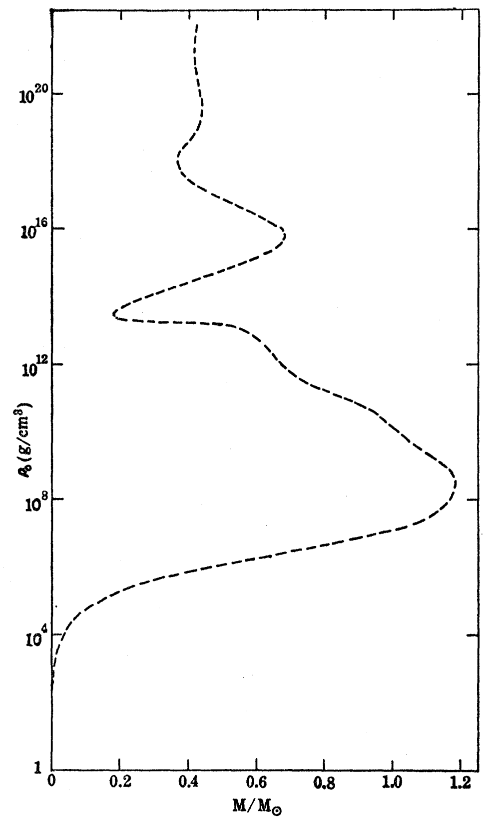

FIG. 6. Graph of total mass of star as function of central density, as calculated with equation of state of Ref. 4. $M_\odot$ = solar mass. Oscillatory behavior at high densities is apparent.

decrease again. Thus ν can never reach $\frac{1}{2}$. ν cannot even approach $\frac{1}{2}$ asymptotically.

For large D_0, we have the same situation as before: the trajectory approximates the ideal trajectory closely. Eventually D becomes large enough for the last term in Eq. (3.19) to dominate. We note that this term has a factor $(1+3\sigma h)(1-2\nu)^{-1}$ which did not occur in Eq. (3.20). However, the first factor must lie between the values $1+3k$ and 1 and cannot affect g much, and the second factor is well behaved as long as ν stays away from $\frac{1}{2}$. This is assured, as noted above. In this way, we see that the extra factors modify the equation for $d\sigma/dx$ in an almost trivial fashion, and we can expect the same qualitative behavior as was exhibited earlier in the approximate case.

We can calculate the period and amplitude of oscillation as before. We obtain a period ($\ln D_0$ is the independent variable)

$$T=8\pi(1+k)/(7+42k-k^2)^{1/2}, \tag{5.1}$$

phase

$$\phi=-\sin^{-1}\left[\frac{1}{4}\left(\frac{7+42k-k^2}{3k+1}\right)^{1/2}\right], \tag{5.2}$$

and amplitude

$$A=\frac{8k}{k^2+6k+1}\left(\frac{3k+1}{7+42k-k^2}\right)^{1/2}D_0^{-(1+3k)/(4+4k)}. \tag{5.3}$$

For $k=\frac{1}{3}$,

$$T=16\pi/(\sqrt{47}), \tag{5.4}$$

$$\phi=-\sin^{-1}(\tfrac{1}{12}\sqrt{94}), \tag{5.5}$$

and

$$A=(18/7\sqrt{94})D_0^{-3/8}. \tag{5.6}$$

As noted before, these values can express only approximate behavior.

6. NUMERICAL CALCULATIONS

As mentioned earlier, calculations using a particular equation of state were shown in graphs in Ref. 4. While the oscillatory behavior of the mass as a function of the central density is somewhat apparent there, the radius shows no such behavior. FORTRAN calculations performed by the author at Los Alamos have elucidated the behavior of the mass and radius for high central densities. The extended graphs are shown in Figs. 6, 7, and 8. It is now clear that the radius oscillates as well as the mass. (The slightly peculiar behavior near $\rho=10^{13}$ g/cm^3 is due to the crushing point there; see the graph of the equation of state in Ref. 4.) The asymptotic values for the mass and the radius are approximately

$$R=6.4\text{ km},$$
$$M=0.42M_\odot.$$

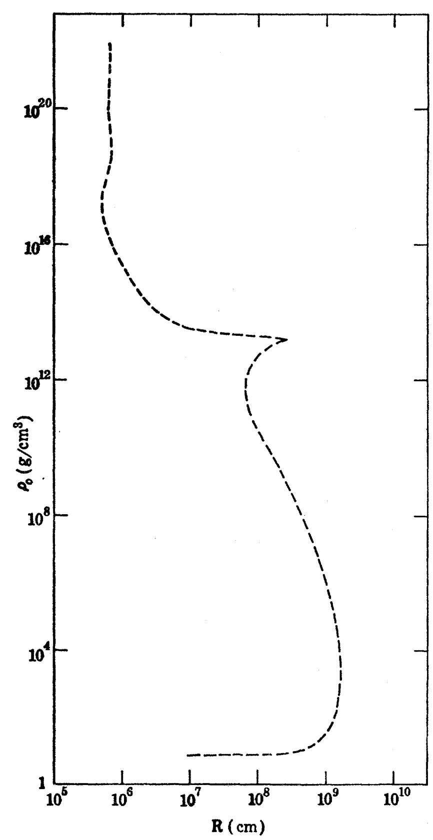

FIG. 7. Graph of radius of star as function of central density, as calculated with equation of state of Ref. 4. Graph oscillates at high densities.

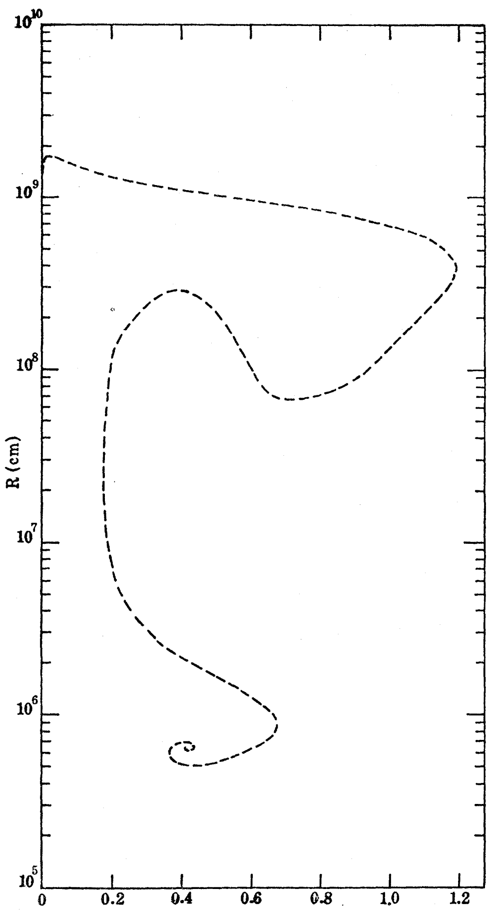

FIG. 8. Graph of radius of star as function of star total mass, as calculated with equation of state of Ref. 4. Central density is parameter along the curve. Note the focal behavior at high densities.

These yield as final values for σ and ν approximately

$$\sigma = 1\times10^{-14},$$
$$\nu = 0.097.$$

The period of oscillation is found to be roughly given by Eq. (5.4) for large D_0.

7. NUCLEON NUMBER

The equation for nucleon number[10,11]

$$dN/dr = 4\pi r^2 n(1-2mr^{-1})^{-1/2}, \quad N(0)=0 \qquad (7.1)$$

was also integrated to determine the total particle number $N(R)$ in the star. In Eq. (7.1), n is the local nucleon density; n must be determined from the equation of state calculations. A convenient analytic fit for $n(\rho)$ for all ranges of ρ was obtained from the calculations used to derive the results of Ref. 4:

$$n = 6.0228\times10^{23}\rho(1+7.7483\times10^{-10}\rho^{9/16})^{-4/9}, \qquad (7.2)$$

where n is in cm^{-3}, ρ in g/cm^3. At low densities, this is the usual proportionality of n and ρ; at high densities, we have $n\sim\rho^{3/4}$.

The calculated results are shown in Fig. 9. It was found most convenient to plot average mass per nucleon, $M(R)/N(R)$, on a scale which shows the deviation from the low-density value; the variable Δm_N is defined as

$$\Delta m_N = \frac{M(R)}{N(R)}\left[\frac{N(R)}{M(R)}\right]_{\text{low-density}} - 1. \qquad (7.3)$$

Thus Δm_N is the binding energy per nucleon in units of nucleon rest energy. It will be noted that, while mass per nucleon remains fairly close to the low-density value, it shows oscillations as D_0 increases, much as the mass does. The oscillations, however, are out of phase with those in the mass; at high densities, they are approximately 180° out of phase.

8. INTERPRETATIONS AND CONCLUSIONS

We first note a fact pointed out by Wheeler[4]: there are regions of instability in the range of central densities. These regions are characterized by $dM/d\rho_0<0$; for if we compress the star further to get a higher ρ_0, it can at the same time eject mass. Compression and

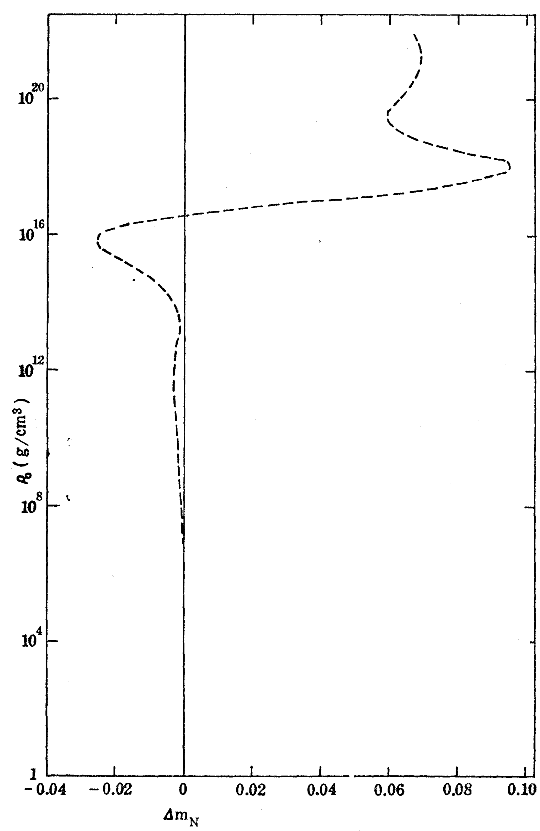

FIG. 9. Graph of relative mass per nucleon as function of central density, as calculated with equation of state of Ref. 4. This is merely the binding energy per nucleon in units of nucleon rest energy: $\Delta m_N = (M/N)[(M/N)_{\text{low density}}]^{-1} - 1$.

simultaneous ejection will then move the star along the curve to a point of minimum mass; further compression would then require augmented mass, so that the star is stable at this point with respect to small perturbations of mass. However, the binding energy curve shows that $\Delta m_N \geq 0$ for $\rho_0 \gtrsim 10^{16}$ g/cm^3, so that the star is unstable against large-scale deformation and complete dispersal into individual particles. The detailed treatment of this stability behavior is presented elsewhere.[11]

The results of this paper are quite insensitive to the exact details of the equation of state. The only assumptions are found in Eqs. (2.11)–(2.12) and in the requirement that $g(D)$ become large for small D. $g(D)$ need not even be monotonic. However, there might be more difficulty in proving the paper's conclusions if g decreases below unity for large D, since the initial slope of the trajectory would become less steep and there would be a tendency for the trajectory to go to the right instead of downward if g were small enough. We can investigate the possibility of this behavior of g. Suppose, for large D, S has the behavior

$$S = kD - AD^{1-\mu} \tag{8.1}$$

with $0 < k \leq 1$, $\mu > 0$, $A > 0$. Then calculation shows that $dg/dD < 0$ (monotonically decreasing) for large D if

$$(1+k)^{-1} > \mu. \tag{8.2}$$

Now, for a mixture of relativistic Fermi gases we find $\mu = \frac{1}{2}$. Equation (8.2) then becomes

$$1 > k. \tag{8.3}$$

This is satisfied for $k = \frac{1}{3}$, as in Ref. 4. Investigation into the case $k = 1$ shows that more terms in Eq. (8.1) are needed to determine the sign of dg/dD. However, even if g should go below unity and then increase to approach unity, the arguments in the text will hold unless g decreased substantially below one, which is extremely unlikely.

The most important quantity to be determined for high-density equations of state is obviously the constant k. There is yet considerable uncertainty as to its value. Reference 4 gives $k = \frac{1}{3}$; Zel'dovich[9] obtains a possible $k = 1$. Ambartsumyan and Saakyan[13] consider the possibility of formation of baryons heavier than nucleons and their results yield a possible value $k = 1/13$, as mentioned in Ref. 10. We can expect the final star mass and radius to depend markedly on k, since the position of the focus in the ideal system is a function of k. The value of ν at the focus for the relativistic equations is $2k(k^2+6k+1)^{-1}$, and this quantity takes the values 1/4, 3/14, and 13/124 for $k = 1$, 1/3, and 1/13, respectively.

[13] V. A. Ambartsumyan and G. S. Saakyan, Astron. Zh. **37**, 193 (1960) [English transl.: Soviet Astron.—AJ 4, 187 (1960)].

One rather striking feature of the results of this paper is the fact that their qualitative behavior does not depend on whether the classical or relativistic equations are used. (Here we speak of the general relativistic equations; special relativity, of course, is used in the equation of state.) The only effect of the inclusion of the general relativistic terms is to modify the numerical results. (A slight exception to this might be found in the above-mentioned situation with $\mu = \frac{1}{2}$, $k = 1$, when the trajectory could have a slight tendency to move out to the right. The relativistic singularity at $\nu = \frac{1}{2}$ would inhibit this tendency.) In connection with this, we mention again that at zero temperature there is no possibility of pathological behavior due to the Schwarzschild "singularity."

The assumption that the temperature $T = 0$ has been made in this paper. It should be noted that the results will hold for $T \neq 0$, as long as T is low enough that the matter is degenerate. Equilibrium cannot be assumed, for there will be radiation from the star; however, there may be quasiequilibrium, since the radiation will change the star's mass appreciably only if it persists over a very long period of time.

We mention briefly the question of conservation of nucleons, raised originally by Wheeler[4] and discussed further by Chiu.[7] In crude form, this problem is: Suppose we have a star near the critical mass limit, and suppose a large amount of mass is gently lowered onto this star. Then the star will become unstable and will tend to eject most of the new mass; however, it does not have enough available energy to do so. The only way in which the star can eject the new mass is to convert nucleons to radiation until enough energy has been acquired to eject the remaining unwanted mass. This violates the law of conservation of baryons. (As emphasized by Chiu, the conversion of nucleons to radiation takes place at the center of the star, where there is a real singularity; the Schwarzschild "singularity" does not contribute to this process.)

There is a tendency to say that this will not happen because of the positive binding energy for $\rho_0 \gtrsim 10^{16}$ g/cm^3. However, we recognize that the positive binding energy will tend to cause gravitational collapse, and Wheeler has shown[11] that, if one compares the endpoint of collapse with the beginning, one has two choices: (1) baryon number is not conserved, or (2) baryon number has no meaning as denoting number of heavy particles. A detailed discussion is given in the reference cited.

ACKNOWLEDGMENTS

This work was carried out under the auspices of the U. S. Atomic Energy Commission. Thanks are due to John A. Wheeler, who made several pertinent suggestions concerning the content of the paper.